Physical and dynamical properties of (12929) 1999 TZ1 suggest that it is a Trojan

A. Moullet, E. Lellouch, A. Doressoundiram, J. L. Ortiz, R. Duffard, A. Morbidelli, P. Vernazza, R. Moreno

A&A 483, L17–L20 (2008)
DOI: 10.1051/0004-6361:200809474

Astronomy & Astrophysics

Letter to the Editor

Physical and dynamical properties of (12929) 1999 TZ_1 suggest that it is a Trojan

A. Moullet[1], E. Lellouch[1], A. Doressoundiram[1], J. L. Ortiz[2], R. Duffard[2], A. Morbidelli[3], P. Vernazza[1], and R. Moreno[1]

[1] LESIA-Observatoire de Paris, 5 place J. Janssen, 92195 Meudon, France
e-mail: arielle.moullet@obspm.fr
[2] CSIC-Instituto de Astrofisíca de Andalusía, Granada, Spain
[3] Observatoire de la Côte d'Azur, Nice, France

Received 28 January 2008 / Accepted 27 March 2008

ABSTRACT

Context. Small body (12929) 1999 TZ_1 is listed by the Minor Planet Center (MPC) as a Centaur. However, its location close to the Lagrangian point L5 of Jupiter is typical of a Trojan object with large inclination.
Aims. The aim of this work is to provide a global physical and dynamical characterization of this object and to reassess its classification.
Methods. We obtained multi-wavelength observations with IRTF (Hawaii), OSN and IRAM-30 m (Spain), and performed a dynamical simulation of the evolution of its orbital parameters.
Results. Visible photometry monitoring shows a rotation curve with a period (if considered double-peaked) of 10.4 ± 0.1 h and an absolute R magnitude $H_R = 9.792 \pm 0.025$. Near-IR spectroscopy indicates a featureless reflectance spectra, with a low spectral slope of 7.2 ± 0.11%/100 nm. Thermal observations at 250 GHz provide a 4.5σ detection with a flux of 1.22 ± 0.27 mJy. The combination of the visible and millimeter datasets, assuming a standard thermal model, leads to a geometric albedo $p_v = 0.053^{+0.015}_{-0.010}$ and a mean diameter of 51.5 ± 5 km.
Conclusions. The low albedo and spectral slope measured are typical of Jupiter's Trojans, but cannot exclude a Centaur nature. However, the dynamical lifetime of the object was estimated to be longer than 1 Gy, which is unlikely for a Centaur and suggests that (12929) 1999 TZ_1 is a Trojan asteroid.

Key words. minor planets, asteroids – radio continuum: solar system – infrared: solar system – celestial mechanics

1. Introduction

Small body (12929) 1999 TZ_1, discovered from Fountain Hills Observatory, Arizona (Juels 1999), appears to be of uncertain nature. Its orbital parameters are: $a = 5.21$ UA, $i = 43.5°$, $e = 0.038$. It has been classified by the MPC among the Centaurs, for no apparent reasons and possibly by error (Spahr, private comm.). According to the latest dynamical nomenclature of outer solar system bodies (Gladman et al. 2008), Centaurs are defined as the non-resonant objects with a semimajor axis included between Jupiter's and Neptune's semimajor axis. They are distinguished from the Jupiter Family comets through conditions on their Tisserand parameter and their perihelion distance. However, the position of (12929) 1999 TZ_1 close to the Lagrangian point L5 could place it among Jupiter's Trojans as well.

Trojans and Centaurs exhibit different stability properties. Trojans form a stable swarm, with long dynamical lifetimes (>1 Gy), while Centaurs are generally unstable (lifetime estimated to be $\sim 10^7$ years, see Tiscareno & Malhotra 2003) and thought to be a reservoir for short-period comets. Centaur objects can also be temporarily captured in Trojan-like orbits (Horner & Wyn Evans 2006), with dynamical lifetimes significantly shorter than those of permanent Trojan objects.

Further distinction between the two populations can also be made from their physical and spectral properties. While Trojans have low geometric albedos, Centaurs exhibit a variety of values from very low to moderate ($p_v = 0.03$–0.18, see Stansberry et al. 2008). In the visible range, Trojan reflectance spectra display low slopes, with little dispersion around the mean value, while Centaur spectral slopes go from very low (flat) to very high (Fornasier et al. 2007). This is less obvious in the IR, where the Centaur spectra tend to flatten. Several ices bands were observed on reflectance spectra of Centaurs (Barucci et al. 2008), while only a few Trojan spectra exhibit mineral bands (Emery & Brown 2003). Trojan spectra are interpreted as belonging to the P or D taxonomic type (Yang & Jewitt 2007).

The detection of water bands in the reflectance spectra, a high geometric albedo (>10%) or a high spectral slope (>15%/100 nm), as well as the discovery of a very dynamically unstable nature (i.e., a short dynamical lifetime on its orbit) would be a strong evidence in favor of a Centaur nature for (12929) 1999 TZ_1. The aim of this work is to provide a physical and dynamical portrait of this object, for which, despite its relative high visual brightness ($\sim V = 17$), no previously published data is available.

2. Optical photometry: rotational light-curve and absolute photometry

Visible observations were carried out with the 1.5 m telescope of Sierra Nevada Observatory (OSN, Granada, Spain), during two campaigns in February and March, 2007. Exact dates and

Table 1. Dates and ephemeris of the (12929) 1999 TZ_1 observations. Integration time refers to the on-source observations. Δ is the geocentric distance, r_h is the heliocentric distance, α is the phase angle.

Telescope and instrument	Date	Integration time (min)	r_h (AU)	Δ (AU)	α (°)
OSN	Feb. 23 (2007)	10	5.318	4.748	9.2
OSN	Feb. 25 (2007)	10	5.317	4.721	9.0
OSN	Mar. 09 (2007)	17	5.314	4.564	7.6
OSN	Mar. 10 (2007)	28	5.314	4.552	7.4
OSN	Mar. 11 (2007)	27	5.314	4.541	7.3
OSN	Mar. 12 (2007)	29	5.313	4.530	7.1
IRAM-30 m, MAMBO	Mar. 30 (2007)	10	5.308	4.370	4.0
IRAM-30 m, MAMBO	Apr. 1 (2007)	30	5.308	4.358	3.7
IRAM-30 m, MAMBO	Apr. 2 (2007)	30	5.308	4.353	3.5
IRAM-30 m, MAMBO	May 25 (2007)	50	5.294	4.502	7.4
IRAM-30 m, MAMBO	May 26 (2007)	20	5.294	4.512	7.5
IRTF, SPEX	Apr. 17 (2006)	40	5.379	4.484	5.3

ephemeris are reported in Table 1. More than 100 exposures of 150 s each were obtained, whose typical seeing ranged from 1.0 to 2.0 arcsec, with median around 1.4 arcsec.

Images were taken using the 2k × 2k CCD camera, with a total field of view of 7.8 × 7.8 arcmin. However, binning 2 × 2 was always used, giving a 0.46 arcsec/pixel scale. This scale was enough to have good point spread function sampling even for the best seeing cases. Because of the object's drift rate (∼10 arcsec/h), we used a short enough exposure time of 150 s to get non-elongated images, but long enough to get a high signal-to-noise ratio for the object. Sky background is then the dominant noise source. The observations were made in the Johnson Cousins *R* filter. The reductions steps are described in Ortiz et al. (2004). The final typical error bars on the individual 150 s integrations were ∼0.02 mag.

The time-resolved observations were inspected for periodicities by means of the Lomb technique (Lomb 1976) as implemented in Press et al. (1992). The Lomb periodogram for the relative photometry shows several peaks. The peak with the highest spectral power (with a confidence level well above 99.99%) corresponds to a periodicity of 5.2 ± 0.1 h (4.62 cycles/day), thus the spin period of this object could be around 5.2 h (if single peaked) or 10.4 h (if double peaked). The double-peaked value is very close to the mean rotation period for Trojans, which is estimated at 11.2 ± 0.6 h in Barucci et al. (2002). The peak-to-peak amplitude of the light-curve is 0.1 ± 0.02 mag (see Fig. 1). From residuals of a sinusoidal fit we get a standard deviation of less than 0.02 mag, consistent with the photometric error estimation. We assume that the light-curve is due to shape effects and thus double-peaked. In this case, since we do not know the rotation axis inclination, we can only infer a minimum difference of 10% between the two main axes of the object. Absolute calibration was obtained in the night of March 11 with Landolt star-field PG 1633+099 and confirmed with USNO-B1 reference stars. It indicated a mean *R* magnitude of 17.23 ± 0.025 mag. To retrieve the absolute magnitude at opposition, we applied the photometric model of Bowell et al. (1989). Using a slope parameter $G = 0.05$ as suggested by Fernández et al. (2003) for Trojans, we obtain $H_R = 9.792$ +/− 0.025 mag. Not even considering that the object is red (see hereafter), this is much fainter than the absolute magnitude $H_V = 9.3$ reported by the Minor Planet Center.

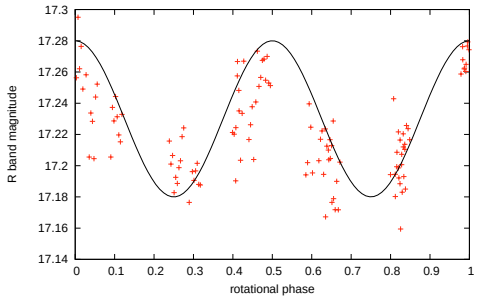

Fig. 1. Optical light-curve of 1999 (12929) TZ_1: *R* magnitude is plotted against rotational phase, for a period of 10.4 h. A sinusoidal fit is overplotted.

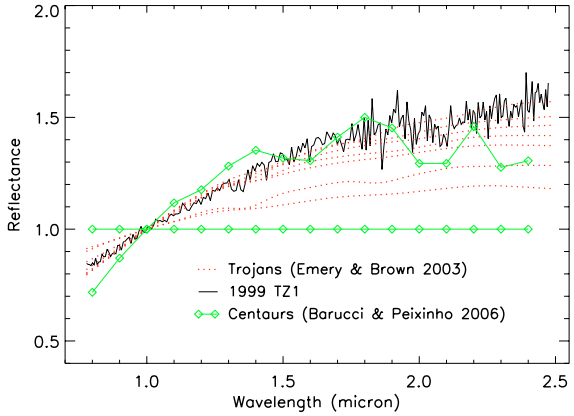

Fig. 2. Reflectance spectrum of (12929) TZ_1 1999 obtained at IRTF, plotted against Trojan spectra from Emery & Brown (2003) and Centaur spectra from Barucci & Peixinho (2006). Objects are (from the flatter spectrum to the steepest): 2060 Chiron, 3793 Leontus, 1437 Diomedes, 4063 Euforbo, 2759 Idomeneus, 3540 Protesilaos, 5254 Ulysses, 624 Hektor, 5145 Pholus. All spectra are normalized to unity at 1 μm.

3. Near-IR spectrometry: reflectance spectra

We obtained a spectrum of (12929) 1999 TZ_1 over 0.7−2.5 μm, using the 3 m NASA Infrared Telescope Facility (IRTF) located on Mauna Kea, Hawaïi. The observations were performed on 2006 April 17, and the average seeing was about 1″.

The instrument SpeX (Rayner et al. 2003) was used in low-resolution prism mode (resolving power $R \sim 100$) to obtain measurements covering the 0.7−2.5 μm range for a total integration time of 2880 s. Signal-to-noise ratio varies from 30 at 2.5 μm to 70 at 0.7 μm. As for visible observations, data were bias and sky-subtracted, then flat-fielded and calibrated in wavelength. The observing and reduction procedures are further described in Vernazza et al. (2007). We transformed our measurements to a solar reflectance spectrum using a nearby solar analog star (HD 102196). Observing circumstances are reported in Table 1. The resulting spectrum (Fig. 2) shows that (12929) 1999 TZ_1 is best classified as a D-type with the near-infrared taxonomy by DeMeo et al. (2007). Indeed its spectrum is characterized by a red slope over the entire wavelength range, constant over 0.8−1.5 μm with a slope value of 7.2 ± 0.11%/100 nm, and an absence of unambiguous absorption features.

If we consider that the reflectance slope is the same in the visible range as in the near-IR (which is usually the case for Trojans), we extrapolate a $V - R$ color of 0.458 ± 0.025 mag. With a mean spectral slope (calculated between *V* and *R*) of 20.601 ± 13.3%/100 nm for the Centaurs and of

7.241 ± 3.9%/100 nm for Trojans (Fornasier et al. 2007), the spectral slope of (12929) 1999 TZ_1 is compatible with both classes, although clearly more similar to the mean Trojan value. As shown in Fig. 2, (12929) 1999 TZ_1's spectrum strongly resembles Trojans spectra observed at the same wavelengths by Emery & Brown (2003), who interpret their spectral slopes as the result of a mixture of silicates, processed organics, and hydrocarbons.

Centaur near-IR spectra display more various slopes, from neutral (Chiron) to very red (Pholus), and several show water ice, methanol, and hydrocarbon ices bands (Barucci et al. 2008). Some Centaur spectra, such as (63252) 2001 BL_{41} (Doressoundiram et al. 2003), appear featureless and/or with relatively low spectral slopes similar to (12929) 1999 TZ_1.

4. Millimeter thermal flux measurement: size and geometric albedo

In order to determine its albedo and size, we observed (12929) 1999 TZ_1 in the thermal range, using the IRAM-30 m MAMBO instrument. Observations were obtained at 5 different dates between March and May 2007 (see Table 1 for details).

MAMBO is a 117-horn array operating at 250 GHz (1.2 mm), which integrates continuum emission on a 60 GHz bandwidth. Each individual bolometer has a 11″ half-power width and is separated from the nearest bolometer by 20″, producing a 240″ wide map. We used an "on-off" observing mode in which the telescope sub-reflector is alternately (with a 2 Hz rate) wobbled between the direction of the source ("on" measurement) and a position 35″ away ("off"). This procedure allowed us to remove most of the sky contribution, but did not eliminate its small temporal fluctuations. The latter can be estimated from the residual sky signal measured in the channels adjacent to the on-source beam. We used 20 min-long on-off integrations that were preceded and followed by pointing and focusing corrections on a strong 12 Jy source (J1256-058). Absolute flux calibration was performed every 2 h on CW-LEO, and accurate atmospheric opacity measurement was obtained every hour (skydip).

Given that we estimated the object thermal flux to be in the 1−2 mJy range, the only goal was to get an unambiguous detection. In particular, and given the low amplitude of the visible light-curve, the search for a thermal light-curve was not possible.

We performed reduction of the MAMBO data within the MOPSIC package in GILDAS environment. The main steps of the reduction are: computation of the "on-off" phases; selection of the best channels in terms of signal-to-noise; calculation of the sky background contribution and variability by looking at spatial and temporal correlations between the various channels. The final result gives a flux of 1.22 ± 0.27 mJy, which corresponds to a 4.5σ detection (see Fig. 3). The 4% absolute calibration error is negligible relative to the detection error bar. Figure 4, which shows the evolution of the signal in each bolometer channel as a function of time, demonstrates that a reliable detection is reached after 3.3 h of integration time.

Combining the thermal and visible fluxes within a thermal model provides a determination of the object size and geometric albedo. Following Fernández et al. (2003), we used a standard thermal model in which the local temperature varies as $T = T_{ss}\cos(SZA)^{0.25}$, where SZA is the solar zenith angle and the sub-solar temperature T_{ss} is expressed as $T_{ss} = [\frac{F(1-A_b)}{\eta\epsilon_b R^2\sigma}]^{1/4}$. Here F is the solar constant, A_b the bolometric albedo, ϵ_b the bolometric emissivity, R the heliocentric distance, and η is a "beaming factor" empirically representing the distribution of surface temperatures and the possible effect of surface roughness. The thermal flux is then equal to $\epsilon_\lambda B_\lambda(T)$, where ϵ_λ is the millimeter emissivity. We assume $\epsilon_\lambda = \epsilon_b = 0.9$. The beaming factor can be determined only if measurements at two or more thermal wavelengths are available. Stansberry et al. (2008) determined a mean $\eta = 1.20$ for Centaurs, while Fernández et al. (2003) obtained $\eta = 0.94$ for Trojans asteroids. Note that for identical surface properties (i.e., rotation rate and thermal inertia), η values are expected to be higher for colder bodies. Here we adopt $\eta = 1$. Finally, we assume a phase integral $q = 0.4$ to calculate A_b, as suggested for low-albedo objects (Lellouch et al. 2000). Although this value is not strictly consistent with our choice of G, this is inconsequential in the low-albedo regime. The object diameter D (in AU) and geometric albedo p are further related to the mean absolute opposition magnitude m_{obj} through $p = (2/D)^2 10^{0.4(m_{sun}-m_{obj})}$, where m_{sun} is the absolute magnitude of the Sun in the same color. Based on physical principles, in this equation the mean opposition magnitude should not include the opposition effect. However, to follow common practice, we used the value derived above from the H-G formalism.

With all these assumptions, we find a mean diameter D = 51.5 ± 5.5 km and a red geometric albedo $p_r = 0.059^{+0.015}_{-0.010}$ in

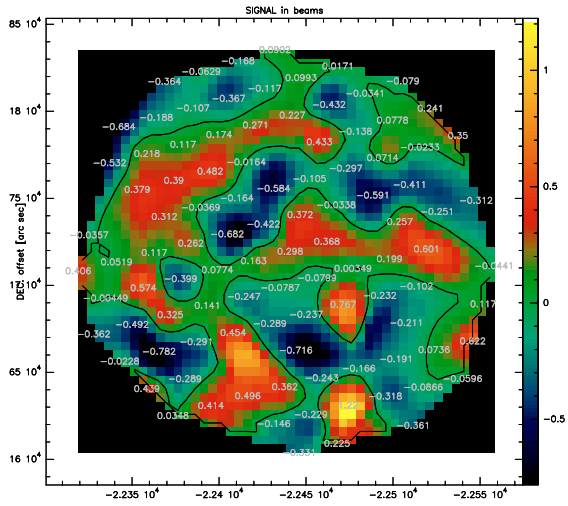

Fig. 3. Flux in mJy/beam measured on the MAMBO array. The source is located at the bottom.

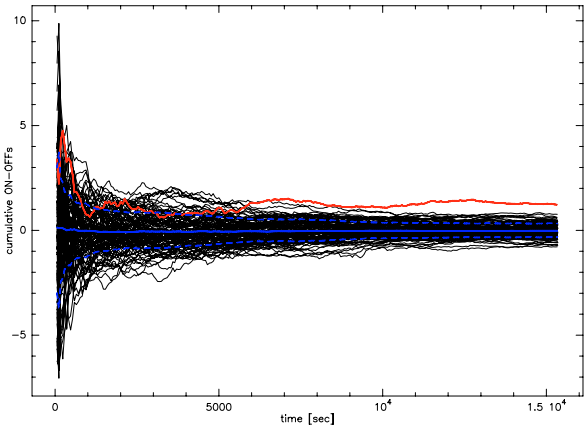

Fig. 4. Signal in mJy/beam for each channel of the bolometer as a function of integration time. The channel pointed on the source is the red one. The blue solid line is the mean signal for all other channels, the blue dotted line is the corresponding 1-σ level.

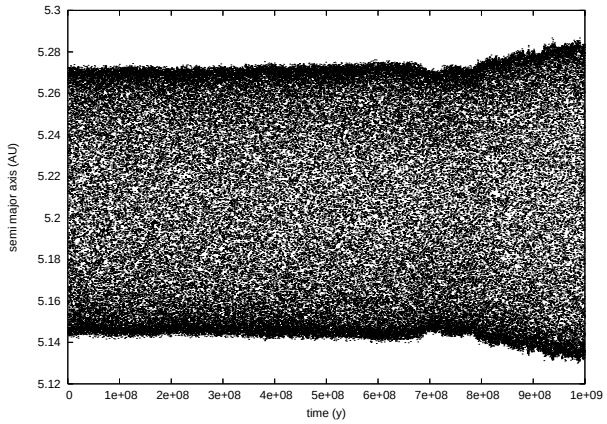

Fig. 5. The time evolution of the semi-major axis of (12929) 1999 TZ_1.

which the error bar is clearly dominated by the error on the thermal flux. Using the previously determined $V-R$ color, we infer $p_v = 0.053^{+0.015}_{-0.010}$. This value is fully consistent with the mean albedo for Trojans found by Fernández et al. (2003) (0.055 ± 0.009). It also matches the mean albedo for Centaurs of 0.065 ± 0.026 determined by Stansberry et al. (2008).

5. Dynamical stability study

We have simulated the evolution of the orbit of (12929) 1999 TZ_1 using the swift_rmvs3 symplectic integrator (Levison & Duncan 1994). Our dynamical model accounts for the four giant planets of the Solar System. The simulation covered 1 Gy, with an integration timestep of 100 days.

Figure 5 shows the evolution of the object's semi-major axis. It oscillates around 5.21 AU during the entire simulation timespan, which makes it undoubtedly a Trojan object. This is also confirmed by the visual inspection of the evolution of the critical angle of the 1:1 resonance $\lambda - \lambda_J$ (not shown in Fig. 5), where λ is the mean longitude and the index $_J$ refers to Jupiter. We note, however, that the amplitude of libration of the semimajor axis is not constant. In particular it increases in the last 300 My of the simulation. Thus, the dynamics of this object is chaotic. This is typical of the long-lived chaotic Trojans with large amplitude of libration (Levison et al. 1997), many of which have lifetimes of the order of billions of years.

Although the chaotic nature of its dynamics cannot exclude that (12929) 1999 TZ_1 is a Centaur recently captured in the 1:1 resonance with Jupiter, we think that this is very unlikely. In the current Solar System, captures of Centaurs for timespans longer than 1 Gy are extremely unlikely. In fact, they have never been observed in numerical simulations (Levison & Duncan 1997; Tiscareno & Malhotra 2003; Horner & Wyn Evans 2006; di Sisto & Brunini 2007). However, the object might have been captured in the Trojan region in the distant past, when the orbital architecture of the giant planets was different. Indeed, it has been proposed (Morbidelli et al. 2005) that all Trojans were former Centaurs, captured ~3.8 Gy ago, during the so-called Late Heavy Bombardment phase of the Solar System, when Jupiter and Saturn crossed their mutual 1:2 resonance. In this case, the different physical properties between Trojans and Centaurs would be explained by the long residence time of the former in the vicinity of the Sun.

6. Conclusions: Trojan vs. Centaur nature

This work led to a detailed portrait of (12929) 1999 TZ_1. We performed near-IR spectroscopy, visible photometry and millimeter observations, bringing information on the absolute optical magnitude, the rotation period, the reflectance spectral slope, the size and the geometric albedo. Spectral slope and geometric albedo appear very close to the mean values for Trojan bodies, i.e., characteristic of a D-type body. This is confirmed by the fact that the reflectance spectrum is featureless. No unambiguous Centaur surface properties were detected. However, since the Centaur dynamical class is very diverse in terms of spectral properties, the physical measurements do not allow us to draw conclusions about the origin of this body.

From a dynamical point of view, (12929) 1999 TZ_1 is a typical Trojan with large amplitude of libration, which exhibits a chaotic behaviour that leads to a slow evolution of the libration amplitude, eccentricity, and inclination. Its dynamical lifetime is of the order of 1 Gy or longer, as it is typical for these objects (Levison et al. 1997).

Acknowledgements. We are grateful to the Sierra Nevada Observatory staff. This research was partially based on data obtained at the Observatorio de Sierra Nevada, which is operated by the Instituto de Astrofísica de Andalucía, CSIC. R.D. acknowledges financial support from the MEC (contract Juan de la Cierva). We thank astronomers and operators at IRAM-30 m antenna who helped during observations, as well as MOPSIC creator R. Zylka who kindly helped with reduction. We also thank C. Thum for allowing extra time to the IRAM observations. IRAM is supported by INSU/CNRS (France), MPG (Germany) and IGN (Spain). We thank J. Emery who kindly shared his data and O. Groussin for interesting discussions. This work was supported by contracts AYA-2004-03250 and AYA2005-07808-C03-01. European FEDER funds for these contracts are also acknowledged.

References

Barucci, M., Brown, M., Emery, J., & Merlin, F. 2008, in The Solar System beyond Neptune, ed. M. A. Barucci et al. (U. of Arizona Press), in press
Barucci, M. A., & Peixinho, N. 2006, in Asteroids, Comets, Meteors, ed. L. Daniela, M. Sylvio Ferraz, & F. J. Angel, IAU Symp., 229, 171
Barucci, M. A., Cruikshank, D. P., Mottola, S., et al. 2002, Asteroids III, 273
Bowell, E., Hapke, B., Domingue, D., et al. 1989, in Asteroids II, ed. R. P. Binzel, T. Gehrels, & M. S. Matthews, 524
DeMeo, F., Binzel, R. P., & Bus, S. J. 2007, in AAS/DPS Abstracts, 39, 35.02
di Sisto, R. P., & Brunini, A. 2007, Icarus, 190, 224
Doressoundiram, A., Tozzi, G. P., Barucci, M. A., et al. 2003, AJ, 125, 2721
Emery, J. P., & Brown, R. H. 2003, Icarus, 164, 104
Fernández, Y. R., Sheppard, S. S., & Jewitt, D. C. 2003, AJ, 126, 1563
Fornasier, S., Dotto, E., Hainaut, O., et al. 2007, Icarus, 190, 622
Gladman, B., Marsden, G., & VanLaerhoven, C. 2008, in The Solar System beyond Neptune, ed. M. A. Barucci et al. (U. of Arizona Press), in press
Horner, J., & Wyn Evans, N. 2006, MNRAS, 367, L20
Juels, C. W. 1999, Minor Planet Circular Orbit Supplement, 47647
Lellouch, E., Laureijs, R., Schmitt, B., et al. 2000, Icarus, 147, 220
Levison, H., Shoemaker, E. M., & Shoemaker, C. S. 1997, Nature, 385, 42
Levison, H. F., & Duncan, M. J. 1994, Icarus, 108, 18
Levison, H. F., & Duncan, M. J. 1997, Icarus, 127, 13
Lomb, N. R. 1976, Ap&SS, 39, 447
Ortiz, J. L., Sota, A., Moreno, R., et al. 2004, A&A, 420, 383
Press, W. H., Teukolsky, S. A., Vetterling, W. T., & Flannery, B. P. 1992, Numerical recipes in C. (Cambridge University Press)
Rayner, J. T., Toomey, D. W., Onaka, P. M., et al. 2003, PASP, 115, 362
Stansberry, J., Grundy, W., Brown, M., et al. 2008, in The Solar System beyond Neptune, ed. M. A. Barucci et al. (U. of Arizona Press), in press
Tiscareno, M. S., & Malhotra, R. 2003, AJ, 126, 3122
Vernazza, P., Rossi, A., Birlan, M., et al. 2007, Icarus, 191, 330
Yang, B., & Jewitt, D. 2007, in AAS/DPS Abstracts, 39, 33.12